

Bulk anisotropic composite rare earth magnets

D. Lee,^{a)} S. Bauser, A. Higgins, C. Chen,^{b)} and S. Liu^{c)}

University of Dayton Magnetics Laboratory, University of Dayton, 300 College Park, Dayton, Ohio 45469

M. Q. Huang

UES Inc., 4401 Dayton-Xenia Road, Dayton, Ohio 45432

Y. G. Peng and D. E. Laughlin

Department of Materials Science and Engineering, Carnegie Mellon University, Pittsburgh, Pennsylvania 15213

(Presented on 31 October 2005; published online 24 April 2006)

Bulk anisotropic composite $\text{Nd}_{13.5}\text{Fe}_{80}\text{Ga}_{0.5}\text{B}_6/\alpha\text{-Fe}$ and $\text{Nd}_{14}\text{Fe}_{79.5}\text{Ga}_{0.5}\text{B}_6/\text{Fe-Co}$ magnets with $(BH)_{\text{max}}=45\text{--}50$ MG Oe have been synthesized by blending a Nd-Fe-Ga-B powder with an $\alpha\text{-Fe}$ or Fe-Co powder followed by hot compaction at 600–700 °C and hot deformation (die upsetting) at 850–950 °C with a height reduction of 71%. The composite $\text{Nd}_{13.5}\text{Fe}_{80}\text{Ga}_{0.5}\text{B}_6/\alpha\text{-Fe}$ and $\text{Nd}_{14}\text{Fe}_{79.5}\text{Ga}_{0.5}\text{B}_6/\text{Fe-Co}$ magnets show microstructures consisting of a very large soft phase up to ~ 50 μm , which is more than 1000 times larger than the upper size limit of the soft phase expected from the existing models of interface exchange coupling. © 2006 American Institute of Physics. [DOI: 10.1063/1.2171959]

I. INTRODUCTION

It is well known that in order to obtain an anisotropic Nd-Fe-B magnet by hot deformation, it is critical to have a Nd-rich phase at the grain boundary in the magnet alloy. It is believed that at the hot deformation temperature (usually around 850–950 °C), the Nd-rich phase is partially melted, which wets grain boundaries and facilitates the formation of the desired crystallographic texture.¹ Yet no Nd-rich phase is present in a composite $\text{Nd}_2\text{Fe}_{14}\text{B}/\alpha\text{-Fe}$ magnet alloy. Rather, a free $\alpha\text{-Fe}$ phase is present. Repeated experiments have demonstrated that it is difficult to obtain good grain alignment in composite $\text{Nd}_2\text{Fe}_{14}\text{B}/\alpha\text{-Fe}$ magnet alloys without the Nd-rich phase.

Previously, bulk anisotropic nanocomposite $\text{Nd}_2\text{Fe}_{14}\text{B}/\alpha\text{-Fe}$ magnets were made by hot compacting and hot deforming two Nd-Fe-B powders, one with a Nd content slightly above the stoichiometric composition (11.76 at %) and the other with a Nd content below the stoichiometric composition. This technique is capable of producing nanocomposite $\text{Nd}_2\text{Fe}_{14}\text{B}/\alpha\text{-Fe}$ magnets with $(BH)_{\text{max}}=40\text{--}45$ MG Oe.² Experiments have established that better magnetic performance can be obtained by substantially reducing the Nd content in the Nd-poor alloy. These results indicate that the best magnetic performance can be accomplished if the Nd content in the Nd-poor alloy is reduced to zero and, thus, the Nd-poor alloy becomes a pure $\alpha\text{-Fe}$ or Fe-B alloy.

II. EXPERIMENT

The purity levels of the raw materials used in our experiments were Nd-95%, Fe > 99%, Co > 99%, and Ga-99.99%. The compositions of the Fe-B alloy were 20.54 wt % B and 77.72 wt % Fe. The particle size of the Fe pow-

der was about 3–5 μm and the O₂ content was 0.2 wt %. The particle size of the 50%Fe–50%Co powder was about 10–50 μm . The Nd-Fe-Ga-B alloys were prepared by vacuum arc melting, followed by melt spinning with a wheel speed of 40 m/s. The ribbons were then crushed to 200–300 μm . Bulk magnet samples were prepared by a two-step process: rf inductive heating to 600–700 °C, along with simultaneous compaction under a pressure of $\sim 1.7 \times 10^8$ Pa for a total cycle time of ~ 2 min, followed by hot deformation (die upsetting) at 850–950 °C under a pressure of $\sim 6.9 \times 10^7$ Pa for a total cycle time of 4–8 min. The typical sample height reduction in the latter step was 71%.

Samples were analyzed using a hysteresis graph for room temperature magnetic properties, using a 13-mm-diam specimen. Scanning electron microscopy (SEM), X-ray diffraction (XRD), and transmission electron microscopy (TEM) were used to characterize particle size, grain alignment, and microstructures.

III. RESULTS AND DISCUSSIONS

Figure 1 is a SEM micrograph showing Fe-Co particles used in this study. Most Fe-Co particles have diameters

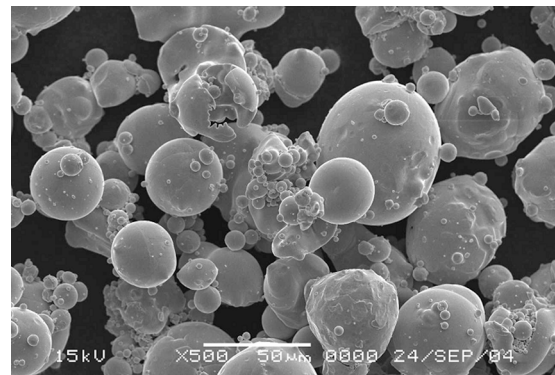


FIG. 1. SEM micrograph of Fe-Co powder particles used in this study.

^{a)}Electronic mail: don.lee@udri.udayton.edu

^{b)}Author to whom correspondence should be addressed; electronic mail: christina.chen@udri.udayton.edu

^{c)}Electronic mail: sam.liu@udri.udayton.edu

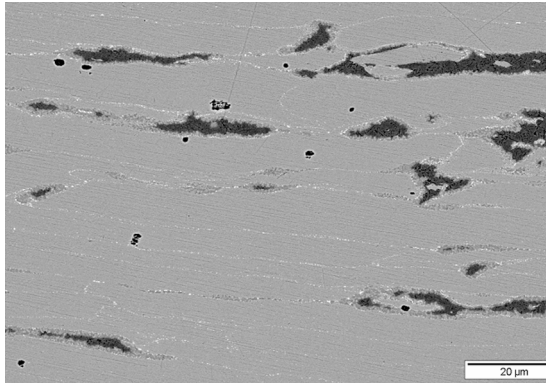


FIG. 2. SEM back scattered electron image of a hot-deformed composite $\text{Nd}_{13.5}\text{Fe}_{80}\text{Ga}_{0.5}\text{B}_6/\alpha\text{-Fe}$ (91.7 wt% / 8.3 wt%) magnet.

ranging from 10 to 50 μm , although particles of only a few micrometers are also present. Similar to the Fe–Co powder, the $\alpha\text{-Fe}$ powder used in this study also has a spherical shape, but with a much small size of 3–5 μm . Figure 2 is a SEM backscattered electron image of a hot-deformed $\text{Nd}_{13.5}\text{Fe}_{80}\text{Ga}_{0.5}\text{B}_6/\alpha\text{-Fe}$ (91.7 wt% / 8.3 wt%) magnet. The dark gray phase is the $\alpha\text{-Fe}$, while the light gray is the 2:14:1 phase. The $\alpha\text{-Fe}$ phase has a length of up to over 20 μm and a thickness of 5–10 μm . Apparently, the $\alpha\text{-Fe}$ powder particles were agglomerated during processing.

Unlike the $\alpha\text{-Fe}$ particles, the Fe–Co particles were not agglomerated. As shown in Fig. 3, each individual Fe–Co phase (the dark gray phase) was formed from a single Fe–Co particle. Composite $\text{Nd}_{14}\text{Fe}_{79.5}\text{Ga}_{0.5}\text{B}_6/\text{Fe-Co}$ magnets demonstrate smooth demagnetization curves with moderately high MH_c of over 10 kOe and $(BH)_{\text{max}}$ up to ~ 50 MG Oe, as shown in Fig. 4. The specimen as shown in Fig. 3 has $MH_c = 10.2$ kOe and $(BH)_{\text{max}} = 46$ MG Oe. Composite Nd–Fe–Ga–B/ $\alpha\text{-Fe}$ magnets show similar demagnetization curves and magnetic performance. As a comparison, the typical magnetic properties of the annealed $\text{Nd}_{14}\text{Fe}_{79.5}\text{Ga}_{0.5}\text{B}_6$ powder were $B_r \approx 8$ kG, $MH_c \approx 17$ kOe, and $(BH)_{\text{max}} \approx 16$ MG Oe.

Adding more soft phase resulted in higher magnetization but lower coercivity. The best magnetic performance was obtained when the Fe–Co or $\alpha\text{-Fe}$ fraction was around 3%–8%. Figure 5 shows the effects of the Fe–Co fraction on the

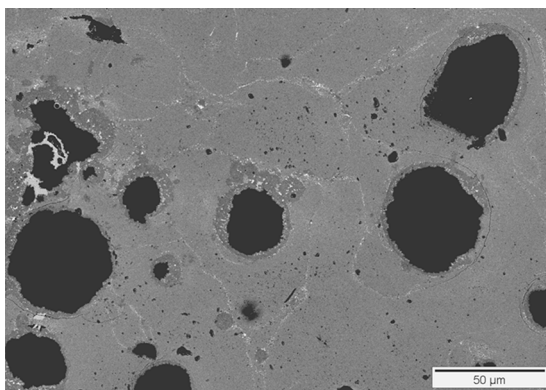


FIG. 3. SEM back scattered electron image of a hot-deformed composite $\text{Nd}_{13.5}\text{Fe}_{80}\text{Ga}_{0.5}\text{B}_6/\text{Fe-Co}$ (95 wt% / 5 wt%) magnet.

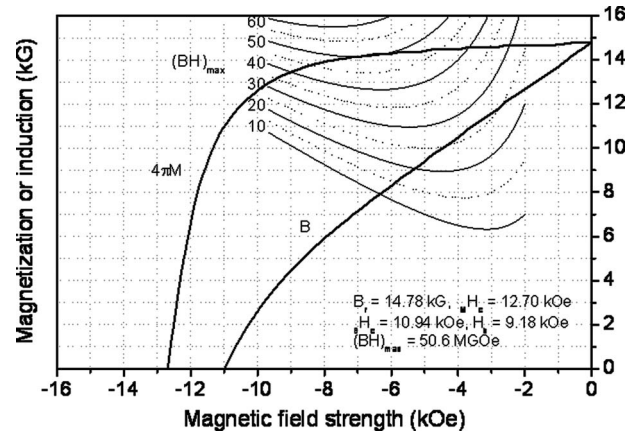


FIG. 4. Demagnetization curves of an anisotropic $\text{Nd}_{14}\text{Fe}_{79.5}\text{Ga}_{0.5}\text{B}_6/\text{Fe-Co}$ (97 wt% / 3 wt%) magnet with $(BH)_{\text{max}} = 50$ MG Oe.

magnetic properties of composite $\text{Nd}_{14}\text{Fe}_{79.5}\text{Ga}_{0.5}\text{B}_6/\text{Fe-Co}$ magnets. A small amount of substitution of Dy for Nd in $\text{Nd}_2\text{Fe}_{14}\text{B}$ led to a substantial enhanced coercivity, which allows adding additional soft phase in the composite magnets, while still maintaining acceptable magnetic properties. For example, a $\text{Nd}_{11}\text{Dy}_3\text{Fe}_{79.5}\text{Ga}_{0.5}\text{B}_6/\alpha\text{-Fe}$ magnet containing 15% $\alpha\text{-Fe}$ phase still demonstrates a high intrinsic coercivity value of over 10 kOe.

Using the technique of blending Nd–Fe–Ga–B with Fe–Co or $\alpha\text{-Fe}$ powder can significantly improve the grain alignment in composite magnets. Figure 6 compares XRD patterns of three magnets. A better grain alignment is represented by enhanced (004), (006), and (008) intensities and a greater than 1 intensity ratio of (006) over (105). It can be seen that the grain alignment of the magnet prepared using blending $\alpha\text{-Fe}$ technique is much better than that of a magnet prepared using blending a Nd-rich alloy and a Nd-poor alloy and similar to that of a commercial sintered anisotropic Nd–Fe–B magnet.

Figure 7 shows elongated and aligned nanograins in the 2:14:1 matrix phase of a $\text{Nd}_{13.5}\text{Fe}_{80}\text{Ga}_{0.5}\text{B}_6/\alpha\text{-Fe}$ (95 wt% / 5 wt%) magnet with $(BH)_{\text{max}} = 48$ MG Oe. Figure 8 shows the hard/soft interface of the same specimen. In addition to elongated and aligned nano- $\text{Nd}_2\text{Fe}_{14}\text{B}$ grains,

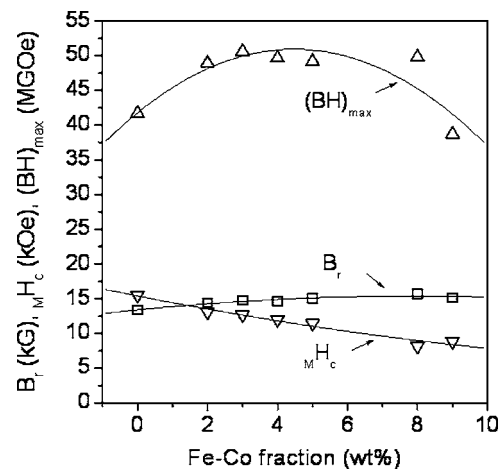


FIG. 5. Effects of Fe–Co fraction on magnetic properties of composite $\text{Nd}_{14}\text{Fe}_{79.5}\text{Ga}_{0.5}\text{B}_6/\text{Fe-Co}$ magnets.

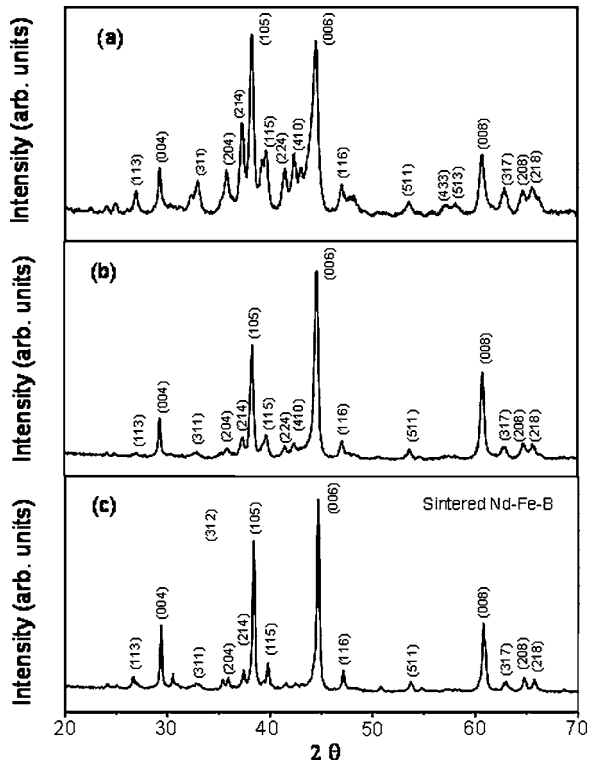


FIG. 6. A comparison of XRD patterns of (a) a composite $\text{Nd}_2\text{Fe}_{14}\text{B}/\alpha\text{-Fe}$ magnet with $(BH)_{\text{max}} \sim 40$ MG Oe prepared by blending a Nd-rich Nd-Fe-B powder with a Nd-poor Nd-Fe-B powder, (b) a composite Nd-Fe-B/ $\alpha\text{-Fe}$ magnet with $(BH)_{\text{max}} \sim 50$ MG Oe prepared by blending a Nd-rich Nd-Fe-B powder with an $\alpha\text{-Fe}$ powder, and (c) a commercial sintered Nd-Fe-B magnet with $(BH)_{\text{max}} \sim 40$ MG Oe.

large $\text{Nd}_2\text{Fe}_{14}\text{B}$ grains are usually observed at the interface, while large $\alpha\text{-Fe}$ particles basically maintain their original round shape after hot deformation.

Previous studies³⁻⁵ reported that the optimum soft phase size in a composite Nd-Fe-B/ $\alpha\text{-Fe}$ magnet is ~ 10 nm and

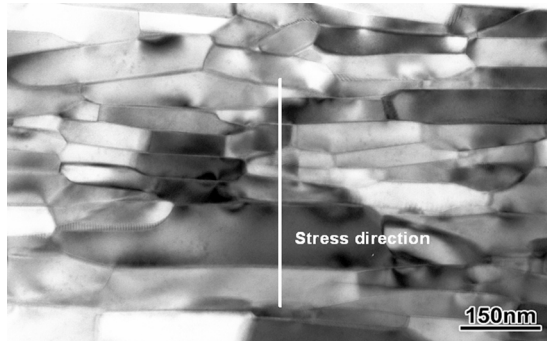


FIG. 7. A TEM micrograph of a $\text{Nd}_{13.5}\text{Fe}_{80}\text{Ga}_{0.5}\text{B}_6/\alpha\text{-Fe}$ (95 wt% 5 wt%) magnet with $(BH)_{\text{max}} = 48$ MG Oe.

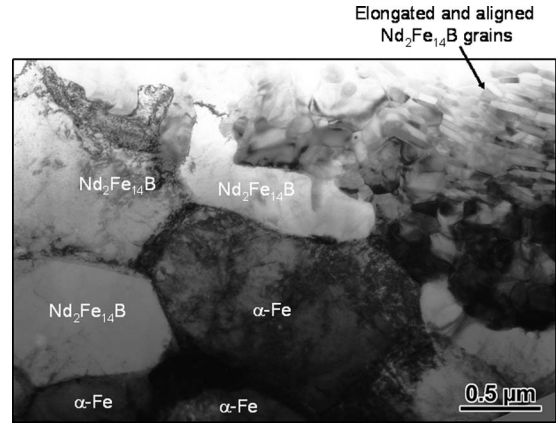


FIG. 8. A TEM micrograph of a composite $\text{Nd}_{13.5}\text{Fe}_{80}\text{Ga}_{0.5}\text{B}_6/\alpha\text{-Fe}$ (95 wt% 5 wt%) magnet showing hard/soft interface.

its upper limit is approximately 20–30 nm for effective interface exchange coupling. However, this study demonstrates that smooth demagnetization curves and high magnetic performance up to 50 MG Oe can be obtained even when the soft phase has very large size up to $50 \mu\text{m}$. This soft phase dimension is more than 1000 times larger than the upper limit of the soft phase size suggested in the current models of interface exchange coupling. This indicates that the hard/soft interface exchange coupling in a composite magnet is actually much stronger than what investigators previously understood.

The microstructures shown in Figs. 2 and 3 are by no means a desired microstructure. If the size of the soft phase can be significantly reduced and its distribution substantially improved, then more soft phase could be added into composite magnets without sacrificing coercivity, which would lead to a greatly enhanced $(BH)_{\text{max}}$.

ACKNOWLEDGMENTS

This study was sponsored by The Defense Advanced Research Projects Agency (DARPA) through ONR under Contract No. N00014-03-01-0636 and through AFRL under Contract No. F33615-01-2-2166. Magnequench MQU-F1 and MQU-F42 powders were used as base line reference materials.

¹J. J. Croat, *Proceedings of the 11th International Workshop on REM*, edited by S. G. Sankar (Carnegie Mellon University, Pittsburgh, PA, 1990), Vol 1, p. 1.

²D. Lee, J. S. Hilton, C. H. Chen, M. Q. Huang, Y. Zhang, G. C. Hadjipanayis, and S. Liu, *IEEE Trans. Magn.* **40**, 2904 (2004).

³E. F. Kneller and R. Hawig, *IEEE Trans. Magn.* **27**, 3588 (1991).

⁴R. Skomski and J. M. D. Coey, *Phys. Rev. B* **48**, 15812 (1993).

⁵A. Manaf, R. A. Buckley, and H. A. Davies, *J. Magn. Magn. Mater.* **128**, 302 (1993).